Glycobiology, 2017, vol. 27, no. 9, 847–860
doi: 10.1093/glycob/cwx041
Advance Access Publication Date: 26 June 2017
Original Article

Cell Biology

Enterocyte glycosylation is responsive to changes in extracellular conditions: implications for membrane functions

Dayoung Park[2,5], Gege Xu[2,5], Mariana Barboza[2,3], Ishita M Shah[4], Maurice Wong[2], Helen Raybould[3], David A Mills[4], and Carlito B Lebrilla[1,2]

[2]Department of Chemistry, [3]Department of Anatomy, Physiology and Cell Biology, and [4]Department of Food Science and Technology, University of California, 1 Shields Ave, Davis, CA 95616, USA

[1]To whom correspondence should be addressed: Tel: +1-530-752-6364; Fax: +1-530-752-8995; e-mail: cblebrilla@ucdavis.edu

[5]These authors contributed equally to this work.

Received 24 February 2017; Revised 1 May 2017; Editorial decision 1 May 2017; Accepted 5 May 2017

Abstract

Epithelial cells in the lining of the intestines play critical roles in maintaining homeostasis while challenged by dynamic and sudden changes in luminal contents. Given the high density of glycosylation that encompasses their extracellular surface, environmental changes may lead to extensive reorganization of membrane-associated glycans. However, neither the molecular details nor the consequences of conditional glycan changes are well understood. Here we assessed the sensitivity of Caco-2 and HT-29 membrane *N*-glycosylation to variations in (i) dietary elements, (ii) microbial fermentation products and (iii) cell culture parameters relevant to intestinal epithelial cell growth and survival. Based on global LC–MS glycomic and statistical analyses, the resulting glycan expression changes were systematic, dependent upon the conditions of each controlled environment. Exposure to short chain fatty acids produced significant increases in fucosylation while further acidification promoted hypersialylation. Notably, among all conditions, increases of high mannose type glycans were identified as a major response when extracellular fructose, galactose and glutamine were independently elevated. To examine the functional consequences of this discrete shift in the displayed glycome, we applied a chemical inhibitor of the glycan processing mannosidase, globally intensifying high mannose expression. The data reveal that upregulation of high mannose glycosylation has detrimental effects on basic intestinal epithelium functions by altering permeability, host–microbe associations and membrane protein activities.

Key words: cell biology, glycosylation, mass spectrometry, membrane proteins, metabolism

Introduction

The large surface area of the gastrointestinal tract provides abundant opportunities for direct contact with substances in the environment. Along its inner wall, at the interface of the intestinal lumen and mucosa, a single layer of epithelial cells mediate the passage of a wide composite of extracellular material, including nutrients from foods, products of microbial fermentation, as well as toxins. Proper growth and vitality of the epithelial monolayer is therefore critical for maintaining a healthy gut. A major proportion of their extracellular membrane proteins are uniquely and densely glycosylated with additions of

saccharide chains. The presented array of glycans is vastly heterogeneous, wherein the degree of branching and composition are governed by the cooperative and nontemplated actions of glycosidases and glycosyltransferases (Aebi et al. 2010). Interruptions of the biosynthetic pathway at the gene or protein levels can potentially alter a multitude of structures that are expressed on the cell surface, which can in turn have long-standing consequences.

Among its explored roles, glycosylation in the gastrointestinal tract fosters host–microbe relationships, providing a source of energy in favor of the colonization of the natural gut flora or pathogens whose glycosyl hydrolases and receptors confer a survival advantage (Moran et al. 2011; Marcobal et al. 2013; Tailford et al. 2015). At a more fundamental level, considerable evidence suggests that the type of glycans presented on proteins participate in regulating key biological processes such as protein folding, stability and localization as well as in determining biological activity (Cumming 1991; Rasmussen 1992; O'Connor and Imperiali 1996; Helenius and Aebi 2001; Moremen et al. 2012; Stowell et al. 2015). Given that a synergistic relationship between glycans and the underlying proteins exists, alterations that occur in intestinal cell surface glycosylation may not only curb or intensify extracellular interactions but also affect the cell's physiology. However, the contributors of intestinal glycosylation changes or the prolonged effects of differential expression are poorly understood. To assess glycan-environment relationships, we selected well established and widely studied human cell lines, Caco-2 and HT-29, which exhibit classical characteristics that model small intestinal absorptive epithelial cells upon reaching confluence (Pinto et al. 1983; Rousset 1986; Hilgers et al. 1990). Controlled changes in media composition, pH and maintenance were made to understand which environmental stimuli significantly alter the intestinal glycosylation machinery. Assessment of these molecular changes is often undetectable under the microscope and requires sensitive analytical tools, which are continuing to be developed for large-scale system-wide studies.

Here we investigated the *N*-glycomic changes that occur on cell surfaces after supplementation with dietary and microbial compounds that are important for intestinal epithelial cell survival and proliferation. Given the nature of culturing cells, we additionally considered the effects of the variable factors in maintenance practices. The results were subsequently used to evaluate the functional consequences of glycan modifications. In concert, our analyses reveal associations between extracellular conditions and membrane glycosylation and delineate the role of *N*-glycan structures in ensuring normal cell functions. This type of screening may help establish regulations that minimize changes to the cellular glycome. In addition, understanding the factors that affect glycosylation complement glycan engineering methods that are currently emerging to tune the cell to produce specified glycan patterns (Elliott et al. 2003; Wurm 2004; Du et al. 2009; Hudak et al. 2011; Sackstein 2012).

Results

Metabolism of dietary components routes glycan expression

We examined whether supplementation of free monosaccharides derived from diet changes *N*-glycosylation outcomes on the intestinal cell surface at concentrations relevant to physiological conditions. Changes in glycosylation were assessed by globally releasing glycans from membrane proteins extracted from fully differentiated (Caco-2) and partially differentiated (HT-29) intestinal epithelial cells and analyzing the mixture by porous graphitized carbon (PGC)–LC–MS. This approach allowed us to derive comprehensive maps encompassing over 300 unique structures and monitor their expression levels individually. The glycan profile under normal growth conditions was used as a frame of reference with which to compare the glycome at varied environments.

Abundant in nearly all carbohydrate-containing foods, glucose (Glc) is a soluble hexose sugar that can be efficiently metabolized by cells (Figure 1) and utilized as a primary energy source. Delivery of glucose to the proximal gut is highly regulated in healthy individuals, keeping intraluminal glucose levels fairly constant regardless of dietary load, ranging from 0.2 to 50 mM in the mammalian small intestine (Ferraris et al. 1990). After high glucose supplementation (25 mM), we observed minimal changes in the groups of glycans presented on Caco-2 across all replicate samples (Table I). Within groups, individual glycan compositions showed no more than 1.7-fold changes (Figure 2A). On HT-29 cells, the abundances of nondecorated complex/hybrid glycans decreased by 20% ($P < 0.05$) following treatment (Table I). However, they constitute a minor component of the cell surface and sum to <4% of the total *N*-glycans. Overall, a high glucose environment did not have a substantial impact on cell surface *N*-glycosylation, indicating that absorbed glucose is ubiquitously interconverted into other activated monosaccharide forms without favoring specific biosynthetic routes (Figure 1). Similar to glucose, mannose (Man) is found in all glycoprotein-containing food products and is equally an important precursor for *N*-glycan synthesis. Predictably, no major changes were observed in Caco-2 cell surface glycans upon treatment with mannose, consistent with the effects observed by glucose treatment (Table I). The lack of discrete changes provides support that exogenous mannose likewise is readily utilized by multiple metabolic routes. In fact, its activated phosphorylated form (Man-6-P) can be converted into all of the monosaccharide constituents transferred onto the nascent *N*-glycan chain (Figure 1). In comparison, HT-29 cells grown in the presence of free mannose showed significant changes ($P < 0.05$) collectively in high mannose type glycans (Table I). When glycan species were evaluated individually, slight increases in Man 3, Man 7 and Man 9 were observed (Figure 2A). This data demonstrates that mannose utilization is better with exogenous mannose than via glucose interconversion, supporting earlier beliefs (Ichikawa et al. 2014).

Although elementally similar to glucose, galactose (Gal), a common component of dairy and plant-based carbohydrates, is not readily metabolized and must first be converted. Unlike the effects observed by glucose treatment, significant increases ($P < 0.05$) were observed for all high mannose (Man 3–Man 9) (Figure 2A) and nondecorated complex/hybrid types of *N*-glycans (e.g. $Hex_5HexNAc_4$ and $Hex_5HexNAc_5$) in galactose-treated Caco-2 cells (Figure 2A). Correspondingly, the relative abundances of fucosylated and sialylated glycans decreased after treatment by 12–28% ($P < 0.05$) (Table I). This effect is shown more clearly by the change in abundances of individual glycans. In untreated controls, afucosylated and asialylated glycans constituted 15 and 23%, respectively, of all complex/hybrid glycans (Figure 2B and **C**). In contrast, the same group made up 46 and 58%, respectively, of all complex/hybrid glycans in galactose-treated cells. To validate the utility of using glycan profiles in describing discrete biological effects, we assessed the reproducibility of each treatment. Glycan profiles of biological replicates after galactose treatment demonstrated high sample and instrument stability (Figure S1).

A derivative of glucose, *N*-acetylglucosamine (GlcNAc) is also found in all glycoprotein food products and involved in the biosynthesis of both CMP-*N*-acetylneuraminic acid (Neu5Ac; NeuAc) and

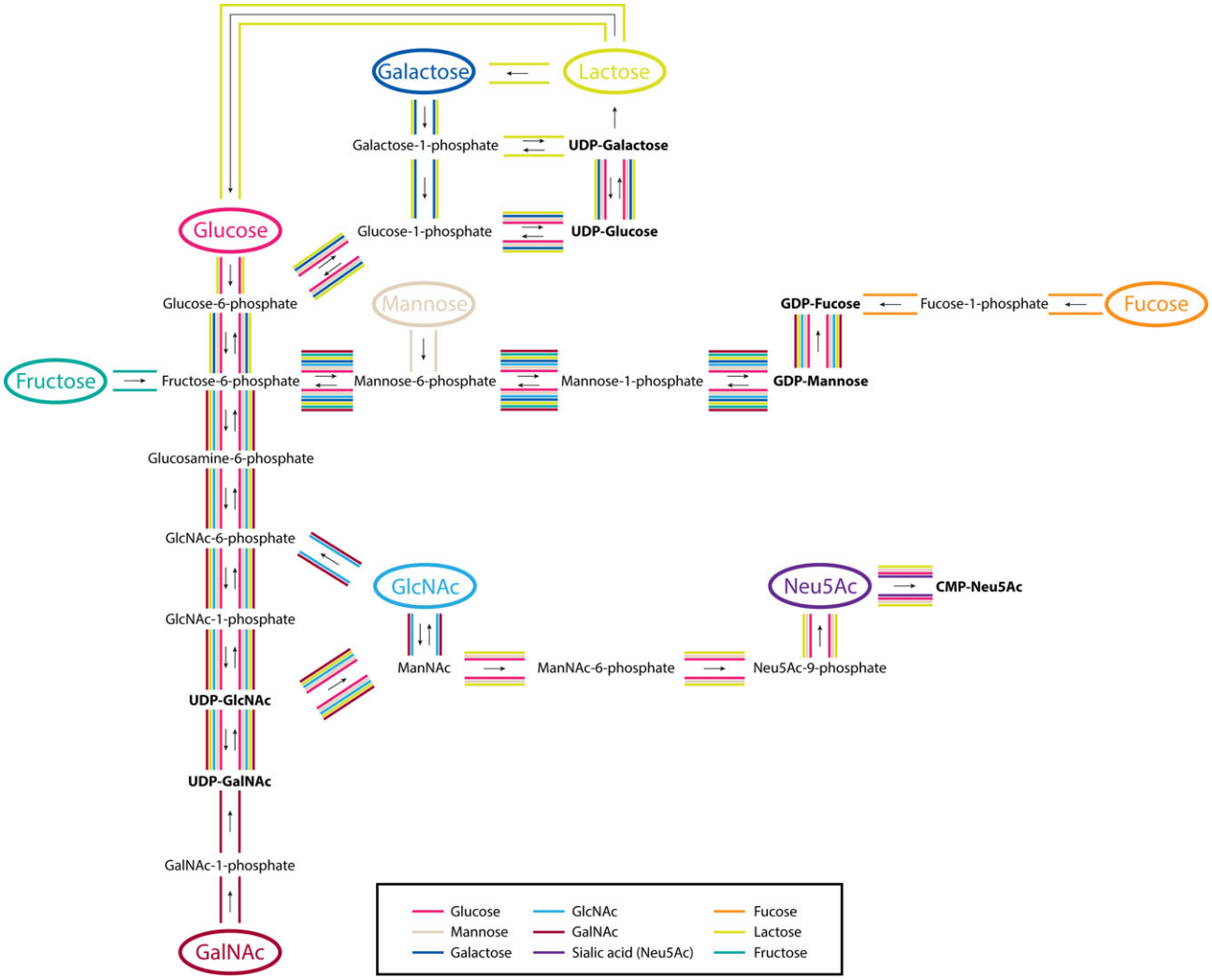

Fig. 1. An outline of the interconversion and activation pathways of exogenously introduced human monosaccharide components of diet. Significant routes from this study are highlighted by colored lines corresponding to each monosaccharide. Activated sugar forms are bold faced. This figure is available in black and white in print and in color at *Glycobiology* online.

GDP-fucose (Fuc) through divergent pathways (Keppler et al. 1999; Snider 2002). When supplemented with 25 mM GlcNAc, fucosylated glycans collectively increased by 61.2% ($P < 0.05$) while sialylated glycans decreased by 53.9% ($P < 0.05$) (Table I). Specifically, cells showed higher expression of monofucosylated types (e.g. $Hex_3HexNAc_5Fuc_1$, $Hex_4HexNAc_5Fuc_1$, $Hex_6HexNAc_7Fuc_1$ and $Hex_6HexNAc_7Fuc_1NeuAc_1$) and lower expression of disialylated structures (e.g. $Hex_5HexNAc_5NeuAc_2$, $Hex_5HexNAc_4NeuAc_2$ and $Hex_5HexNAc_4Fuc_1NeuAc_2$) (Figure 2A–C). These results show that formation of GDP-Fuc is likely favored over CMP-Neu5Ac when excess extracellular GlcNAc is supplied to cells (Figure 1). Closely integrated into GlcNAc metabolism, the monosaccharide *N*-acetylgalactosamine (GalNAc) may also partake in glycoprotein synthesis through the conversion of UDP-GalNAc to UDP-GlcNAc. In support of this route, the glycan changes observed after GalNAc addition resembled those observed on GlcNAc-treated cells, where the abundances of fucose-containing structures increased (120%, $P < 0.05$) and the abundances of sialic acid-containing structures decreased (31.8%, $P < 0.05$) (Table I). Compared with GlcNAc, changes resulting from GalNAc supplementation were more intense for purely fucosylated species. This effect is predominantly attributable to the heightened expression of two core-fucosylated, agalactosylated compounds, $Hex_3HexNAc_4Fuc_1$ and $Hex_3HexNAc_5Fuc_1$, which increased 13- and 7-fold, respectively (Figure 2A). Contrary to GlcNAc treatment, addition of GalNAc resulted in a marked increase in nondecorated complex/hybrid structures (234%, $P < 0.05$), particularly of a biantennary compound, $Hex_5HexNAc_4$ (Table I).

We next investigated how L-fucose, the only levorotatory monosaccharide utilized by mammalian systems, is incorporated onto glycoproteins from extracellular sources. When Caco-2 cells were supplemented with high concentrations (25 mM) of fucose, neither the total levels nor the degree of fucosylation deviated significantly from what was observed in the control (Table I and Figure 2B). Based on compound-by-compound analysis, we found a select group of fucosylated structures that increased, including $Hex_4HexNAc_5Fuc_1$, $Hex_5HexNAc_5Fuc_2$ and $Hex_3HexNAc_6Fuc_1$ (Figure 2A). We observed a parallel decrease in select fucosylated structures that were also sialylated (e.g. $Hex_6HexNAc_4Fuc_1NeuAc_1$ and $Hex_6HexNAc_7Fuc_1NeuAc_1$). In complement, an overall decrease in sialylated glycans accompanied treatment (Table I). The earlier observations that mannose, GlcNAc and

Table I. Percent changes in abundances of cell surface glycans on Caco-2 and HT-29 after addition of supplements. Columns are grouped according to glycan type. Significant changes (control to treated) are indicated by colored arrows

	HM[a]		C/H		C/H-F		C/H-S		C/H-FS	
	Caco-2 (%)	HT-29 (%)	Caco-2 (%)	HT-29 (%)	Caco-2 (%)	HT-29 (%)	Caco-2 (%)	HT-29 (%)	Caco-2 (%)	HT-29 (%)
Glutamine 10 mM	↑507[b]	↑39.8	↑467	↑64.2	↑25.5	↑27.4	↓25.7	↓2.6	↓47.1	↓15.0
Glutathione 2 mM	↑0.1	↑37.1	↑9.1	↓10.0	↓1.5	↓6.1	↓21.3	↓0.5	↑2.6	↑1.8
Glutamate 2 mM	↓12.2	↓2.9	↓12.9	↓56.6	↓0.4	↓44.4	↓10.1	↑5.7	↑2.3	↑16.3
Fructose 50 mM	↑511	↑8.3	↑672	↓42.3	↑28.3	↓32.7	↓29.6	↑3.2	↓49.7	↑11.8
Lactose 70 mg/mL	↑6.3		↑26.8		↓20.5		↑37.7		↓0.6	
Glucose 25 mM	↑5.8	↓4.5	↑5.5	↓20.0	↓0.7	↓13.9	↑1.1	↑5.1	ND	↑6.7
Mannose 25 mM	↓8.7	↑53.6	↓17.6	↓13.9	↑16.9	↓12.1	↓1.7	↑10.7	↓3.3	↓0.3
Galactose 25 mM	↑125		↑88.8		↓20.4		↓12.3		↓28.3	
Fucose 25 mM	↓50.9		↓91.0		↑19.5		↓39.7		↑7.4	
GlcNAc 25 mM	↓0.7		↑24.8		↑61.2		↓53.9		↓9.4	
GalNAc 25 mM	↑17.3		↑234		↑120		↓31.8		↓27.5	
Ac5-Sia 10 mM	↑4.2		↑8.0		↑11.7		↓12.8		↓3.5	
Sialic acid 25 mM	↓97.1	↑162	↓100	↑103	↓74.7	↓9.3	↑698	↑120	↓72.3	↓71.0
Acetic acid 50 mM	↓82.1	↑353	↑731	↑98.6	↓42.9	↓32.1	↑655	↑117	↓70.3	↓75.4
Acetic acid 10 mM	↑65.8	↑73.3	↑159	↑59.7	↑60.0	↑35.4	↓8.8	↓11.7	↓26.4	↓2.6
Lactic acid 10 mM	↑25.3	↓2.9	↑103	↑18.8	↑41.6	↑4.6	↓3.3	↑5.3	↓17.7	↓5.0
Butyric acid 10 mM	↑27.1	↑171	↑54.4	↑66.7	↑72.3	↑262	↓31.9	↓39.7	↓12.1	↓28.6

[a]HM, high mannose; C, complex; H, hybrid; F, fucosylated; S, sialylated; ND, no change detected.

[b]Red and blue arrows indicate statistically significant (two-tailed, unpaired Student's *t*-test, $P < 0.05$) increases and decreases in relative abundances compared to untreated controls, respectively. This table is available in black and white in print and in color at *Glycobiology* online.

GalNAc addition affects the production of fucosylated glycoproteins indicates that cytosolic activation to GDP-Fuc does in fact occur in Caco-2 and HT-29 cells. Together, these results support the metabolic pathway wherein fucose is not rapidly converted into other activated monosaccharide forms (Figure 1).

Among the most structurally unique and widely studied monosaccharides, sialic acids (Neu5Ac; NeuAc; Sia) are metabolically produced by condensation of phosphorylated *N*-acetylmannosamine (ManNAc-6-P) (Figure 1). Although free sialic acids are present in nature, diffusion across the membrane is limited due to their anionic charge and most exist as oligo-*O*-acetylated forms. Therefore, in this study, we utilized per-*O*-acetylated sialic acid (2,4,7,8,9-penta-*O*-acetyl *N*-acetylneuraminic acid (Ac5-Sia)) in concentrations of up to 10 mM. After 72 h, the abundances of sialylated compounds remained relatively unchanged compared to untreated controls. On the contrary, significant increases ($P < 0.05$) were observed for monofucosylated glycans (Figure 2B), primarily for agalactosylated compounds, $Hex_3HexNAc_3Fuc_1$ and $Hex_3HexNAc_6Fuc_1$ (Figure 2A).

Besides the common monosaccharide building blocks found in glycosylated products, we assessed the effects of fructose, a major ingredient in foods that have high sugar content. Fructose availability in the gut is greatly affected by diet. Luminal fructose concentration in rats fed with high fructose diet was reported to be 26 mM or higher (Kirchner et al. 2008). Strikingly, Caco-2 growth in high fructose (50 mM) environments resulted in significant increases ($P < 0.05$) in the concentrations of high mannose and nondecorated complex/hybrid type *N*-glycans, producing abundance changes of 511 and 672%, respectively (Table I). The same upregulation was observed for monofucosylated, asialylated glycans that contain less than five GlcNAc residues (Figure 2A). These include $Hex_3HexNAc_4Fuc_1$, $Hex_4HexNAc_5Fuc_1$, $Hex_6HexNAc_4Fuc_1$ and $Hex_5HexNAc_5Fuc_1$, which each increased more than 4-fold. When taken up by cells, fructose is converted to fructose-6-phosphate, which can then be incorporated onto cell surface glycoproteins by conversion to a variety of monosaccharide donors such as UDP-Glc, UDP-GlcNAc and GDP-Man (Snider 2002) (Figure 1). In Caco-2, fructose supplementation favored mannosylation. While exogenous fructose directly participates in de novo glycan biosynthesis, utilization varies by cell type. In contrast to Caco-2, the majority of high mannose and fucosylated glycans in HT-29 cells remained unaltered (Figure 2A).

Given that monosaccharides from exogenous sources directly participate in the glycosylation pathway, we next determined whether their naturally glycosylated forms have similar metabolic fates upon uptake. Lactose, the major component of milk, is a disaccharide sugar composed of glucose and galactose linked by a beta glycoside bond, which upon consumption can be cleaved by intestinal epithelial cells into the respective monosaccharide parts (Figure 1). When we supplemented Caco-2 with lactose (70 mg/mL), most types of complex/hybrid *N*-glycans changed following the same trends as under high galactose conditions (Table I). For example, fucosylated compounds significantly decreased by 20% ($P < 0.05$) in both cases. However, unlike galactose treatment, addition of lactose did not cause dramatic changes in high mannose glycosylation. At the individual, single compound level, meaningful changes in abundances were solely observed in complex or hybrid type glycans that possessed at least one galactose residue (Figure 2A).

Microbial byproducts create glycan-altering environments

During fermentation of dietary fibers, gut microbes produce short chain fatty acids (SCFAs), which are readily absorbed by colonocytes. SCFA concentrations vary longitudinally along the intestines, ranging from 20 to 40 mM in the terminal ileum, 70 to 140 mM in the proximal colon and 20 to 70 mM in the distal colon (Cummings et al. 1987; Nastasi et al. 2015). To examine the effects of microbial byproducts on intestinal epithelial glycosylation, we supplemented cells separately with acetate (C2), lactate (C3) and butyrate (C4) to a final concentration of 10 mM. In total, a significant increase in fucosylated glycans ($P < 0.05$) accompanied treatment of Caco-2 cells

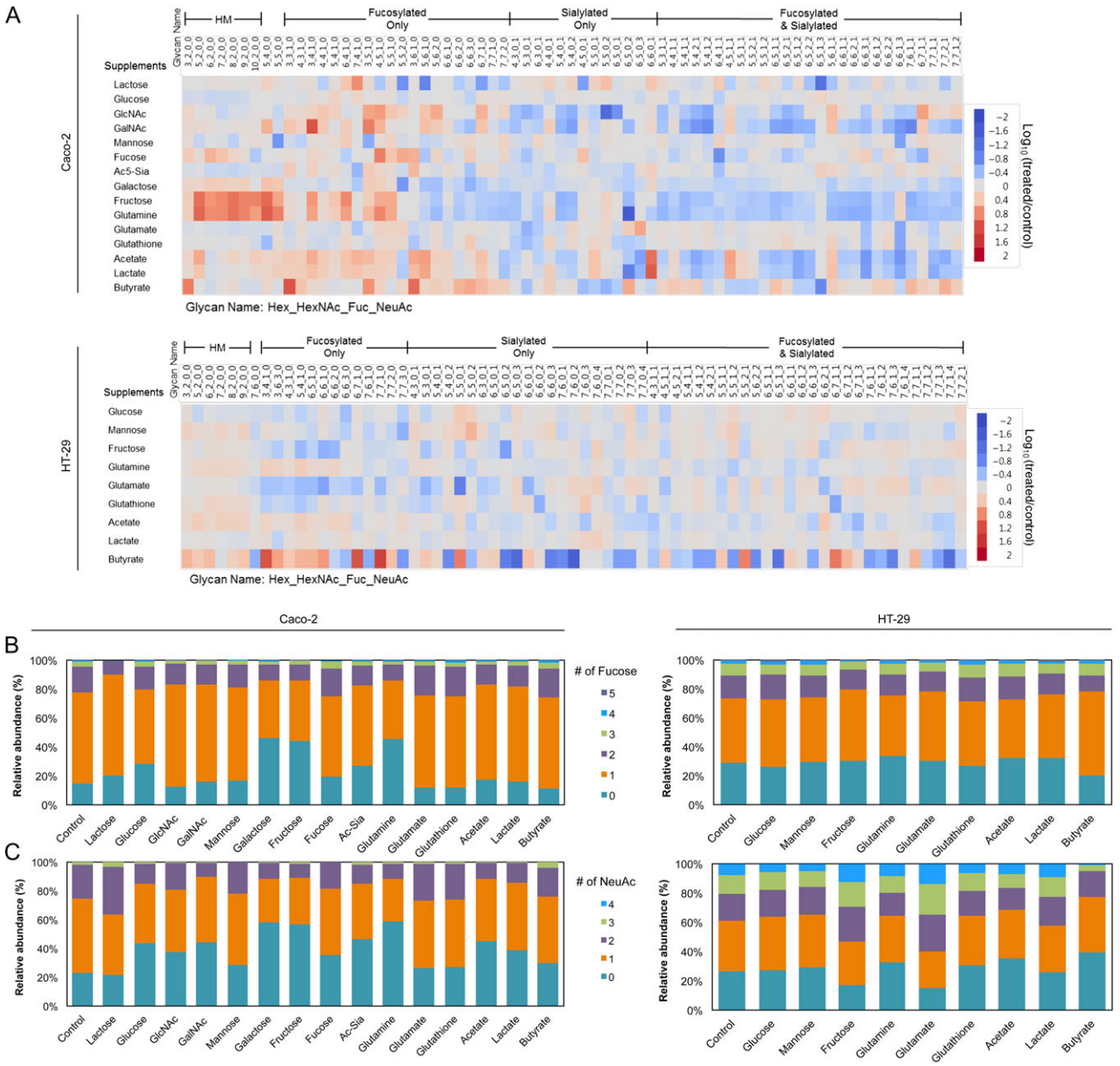

Fig. 2. Changes in Caco-2 and HT-29 cell surface glycan abundances following supplementation. (**A**) Heatmap of altered glycan compositions from untreated to treated Caco-2 and HT-29 cells. A threshold of relative abundances >0.5% and fold changes >2 was used. Data are represented as the log value of the fold change. Glycan mass increases from left to right within each group. Naming is as follows: Hex_HexNAc_Fuc_NeuAc. (**B** and **C**) Relative distribution of fucosylation and sialylation in Caco-2 and HT-29 cells after treatment. Each feature is separated according to number of residues. This figure is available in black and white in print and in color at *Glycobiology* online.

with each SCFA (Table I). In examining individual glycan compositions, we observed that the consequences of acetate and lactate treatments on Caco-2 were comparable, particularly for branched sialylated structures. Among these, distinguishable glycans include $Hex_6HexNAc_6NeuAc_1$, which increased with treatment (8.1-fold with acetate; 10-fold with lactate), as well as $Hex_6HexNAc_6Fuc_1NeuAc_3$ and $Hex_7HexNAc_7Fuc_1NeuAc_1$, which decreased with treatment (4.7- and 2.7-fold, respectively, with acetate; 3.7- and 3.4-fold, respectively, with lactate) (Figure 2A). The changes in sialylated structures produced by butyrate, on the other hand, opposed those produced by acetate and lactate. This contrast is illustrated, for example, in the expression of glycans $Hex_6HexNAc_6NeuAc_1$, $Hex_6HexNAc_5NeuAc_2$ and $Hex_6HexNAc_5Hex_1NeuAc_3$.

Acetate treatment resulted in similar shifts in the HT-29 glycome. However, lactate had minimal effects (Table I). Of the SCFAs, the influence of butyrate was strikingly more dramatic on HT-29 cells than on Caco-2. Upon treatment, fucosylation increased by 262% ($P < 0.05$) (Table I). Monofucosylated glycans were among the structures that showed the greatest change (Figure 2B). Specifically, $Hex_3HexNAc_4Fuc_1$, $Hex_6HexNAc_7Fuc_1$ and $Hex_7HexNAc_7Fuc_1$ each increased more than 13-fold (Figure 2A). In parallel, di- and trisialylated glycans (e.g. $Hex_6HexNAc_5NeuAc_3$, $Hex_7HexNAc_6NeuAc_2$ and

$Hex_6HexNAc_5Fuc_1NeuAc_3$) decreased considerably in abundances in the presence of butyrate (Figure 2A and C).

Noncarbohydrate health supplements integrate into glycan biosynthesis

Intestinal epithelial cells can obtain energy from other noncarbohydrate sources. The amino acid L-glutamine is the major bioenergetic substrate necessary for cell proliferation and survival. Additionally, oral and enteral administration of glutamine-rich formulations has been shown to attenuate gut dysfunction and reduce septic morbidity (Klimberg et al. 1990; van der Hulst et al. 1993). Glutamine is obligate for cell growth in vitro, usually in concentrations of 2–6 mM. When cells were supplemented with high glutamine (10 mM), significant increases ($P < 0.05$) in high mannose, fucosylated and nondecorated complex/hybrid types of glycans were detected in both Caco-2 and HT-29 cells (Table I). Representative chromatograms of identified glycans from Caco-2 cells cultured in normal and high glutamine environments are shown in Figure 3A and B, respectively. According to relative abundances, high mannose type glycans collectively increased by 507% after treatment. Individually, Man 5–Man 9 each increased more than 6-fold (Figure 2A). In addition, we observed elevation of core-fucosylated glycans $Hex_3HexNAc_4Fuc_1$, $Hex_6HexNAc_4Fuc_1$, $Hex_4HexNAc_5Fuc_1$ and $Hex_5HexNAc_5Fuc_1$. Contrastingly, larger fucosylated glycans with more than six HexNAc residues decreased. Sialylated glycans showed remarkable constancy following treatment (Figure 3A and B). According to absolute abundances, the summed abundances of all sialylated glycans in glutamine-treated cells and untreated controls were equal (Figure S2).

In most cells, an immediate product of glutamine metabolism is glutamate. Uptake of glutamate accordingly correlates with decreased paracellular hyperpermeability and supports the protective effects of glutamine but also serves as an oxidative substrate within enterocytes (Blachier et al. 2009; Vermeulen et al. 2011). Jejunal luminal content of glutamate was found to change with diet, elevating to as high as 2.6 mM in healthy human volunteers after a protein-rich meal (Adibi and Mercer 1973). Interestingly, additions of glutamate (2 mM) caused changes in cell surface glycan expression that were unique to HT-29 but in a manner opposite to the effects of glutamine. In particular, a decline in fucosylation was measured with respect to the control (44.4%, $P < 0.05$), mostly affecting monofucosylated structures (Table I). High mannose glycan expression was unperturbed. Cell surface glycans presented on Caco-2 were relatively unaffected by glutamate treatment.

Another vital contributor to normal gut barrier function is glutathione, a water soluble, thiol-containing tripeptide (Glu-Cys-Gly) with antioxidant activity. It is present in intestinal luminal contents at base levels of 0.5 mM, originating chiefly from biliary secretions, but can increase with dietary inclusion, typically at concentrations of 2 mM (Jones et al. 1992). When we examined the impact of the addition of glutathione (2 mM), the expression levels of the major groups of glycans were essentially unaltered (Table I). Only minor decreases were observed exclusively in complex/hybrid glycans with more than five hexose residues ($Hex_6HexNAc_6Fuc_1NeuAc_3$, $Hex_6HexNAc_6Fuc_3NeuAc_1$, $Hex_5HexNAc_3NeuAc_1$ and $Hex_5HexNAc_4$ on Caco-2; $Hex_6HexNAc_7Fuc_1NeuAc_1$ and $Hex_6HexNAc_6NeuAc_2$ on HT-29) (Figure 2A). Such glycosylation changes closely resembled those produced by glutamate. On HT-29, high mannose type glycans increased by 37.1% ($P < 0.05$), an effect

Extracellular acidification remodels the glycome

Oscillations in pH can occur when transport or metabolism is challenged. To evaluate the effects of abnormal pH on cell surface glycosylation, we acidified the growing media to a final pH of 4.5–4.6 using acetic acid (pKa 4.75) and sialic acid (pKa 2.6). The profiles of membrane glycans illustrate the striking redistribution toward purely sialylated compounds in cells grown at low pH compared to cells grown at neutral pH (Figure 3A and C). Interestingly, only a particular subset of sialylated structures was altered. Glycans that showed greater than 3-fold expression changes after addition of acetic acid and sialic acid include mono- or nonfucosylated sialylated structures ranging from one to three sialic acid residues (Figure 4B). While abundant at acidic pH, these same structures were absent or otherwise expressed in minute levels in cells grown in neutral pH. This effect was observed regardless of the acid used to acidify the media. We have previously demonstrated high reproducibility of our method in the detection of sialylated glycans without the need for derivatization (Hua et al. 2011; Ruhaak et al. 2013). Verification of glycan identifications was performed using MS/MS. The annotated spectra of multiply sialylated glycans are shown in Figure S3.

Cell glycosylation is sensitive to growth conditions

To further understand the causal factors of glycan changes, we evaluated the effects that the growing conditions have on cell surface *N*-glycosylation. Different environments are created by changes to the components of the growth medium. Caco-2 cell growth is supported in formulations such as Eagle's Minimum Essential Media (EMEM) and Dulbecco's Modified Eagle's Medium (DMEM). However, DMEM contains two to four times the concentration of amino acids (including glutamine), vitamins, ferric nitrate and sodium pyruvate as EMEM, as well as higher amounts of glucose. To evaluate the influence of the basal media on cell surface glycosylation, we cultured Caco-2 cells separately in either EMEM or DMEM for the first 10 passages and analyzed the *N*-glycans at passage 11 in triplicates. Generally, DMEM-cultured cells showed significant increases ($P < 0.05$) in fucosylated and nondecorated complex/hybrid type glycans, similar to cells supplemented with 10 mM glutamine (Figure S4). In particular, truncated fucosylated structures (e.g. $Hex_3HexNAc_4Fuc_1$) showed the most prominent increase. Contrastingly, high mannose type glycans did not increase as they did under high glutamine conditions. Differences in concentration and composition of the growth media alone led to distinct changes in glycan expression, supporting the observation that membrane glycosylation is impacted by the cell's environment.

Depletions of growth supplies during cell culture have implications on the glycosylation machinery. To account for this factor, Caco-2 cells were grown for at least twelve consecutive passages separately either with media renewal twice or three times a week. In general, glycan samples prepared from Caco-2 cells where media was changed two times a week showed wider variability between biological replicates than cells where media was changed three times a week (Figure 4A). Despite the variations, we consistently observed that the level of high mannose type glycans increased up to 6.5-fold with less frequent media changes (Figure 4A, left panel). Another distinguishing feature between cells was the increase in the abundances of select core-fucosylated glycans, $Hex_3HexNAc_4Fuc_1$, $Hex_4HexNAc_5Fuc_1$, $Hex_5HexNAc_5Fuc_1$ and $Hex_6HexNAc_4Fuc_1$ (Figure 4A, right panel).

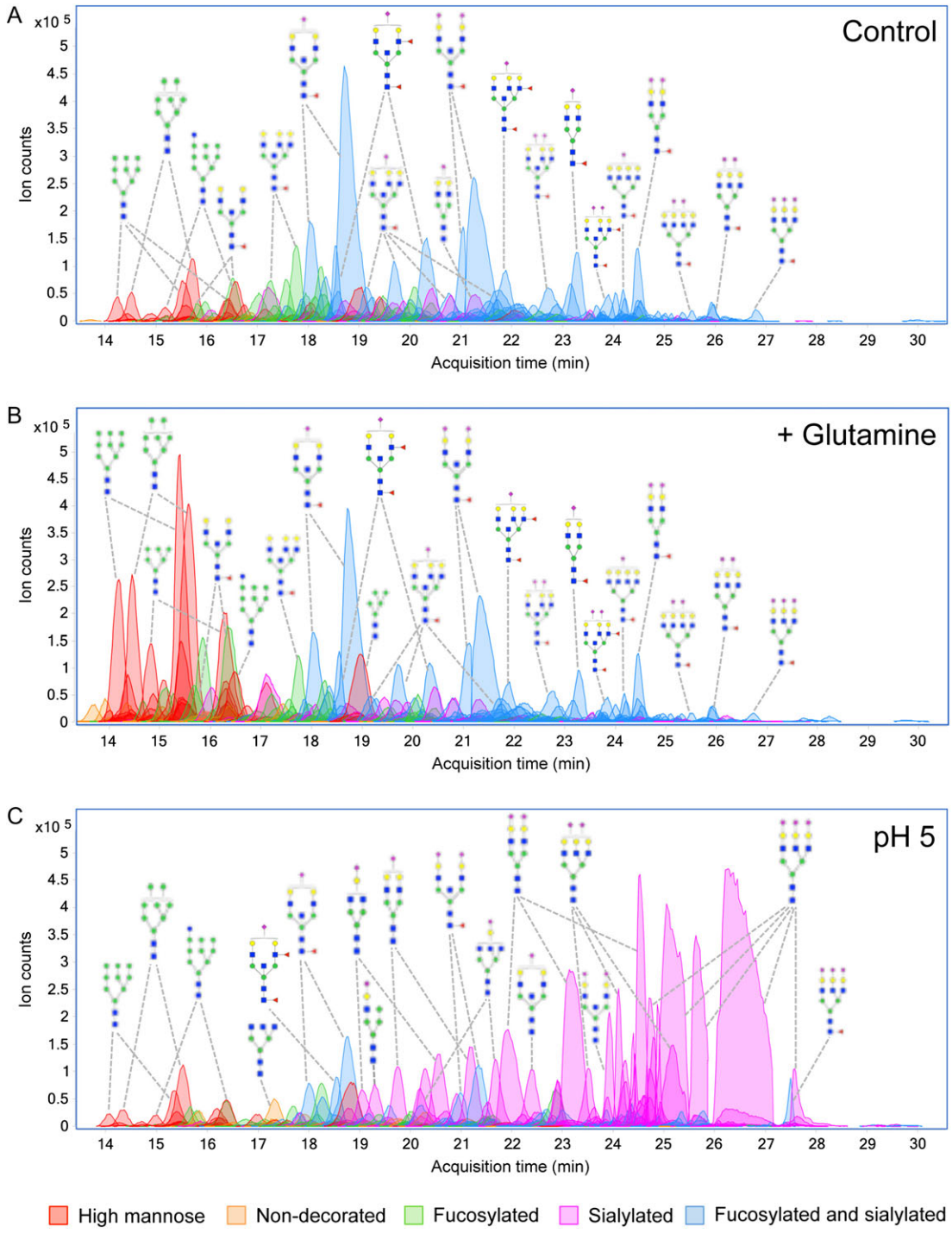

Fig. 3. Chromatogram of identified cell surface glycans released from Caco-2. Profiles are shown for (**A**) Caco-2 untreated, (**B**) Caco-2 after addition of glutamine and (**C**) Caco-2 grown under low pH with addition of acetic acid. Monosaccharide symbols follow the Symbol Nomenclature for Glycans (SNFG) system details at NCBI (Varki et al. 2015). This figure is available in black and white in print and in color at *Glycobiology* online.

An inherent variability between experiments is passage number, or the number of times cell populations have been subcultured. The use of high passage cells has been reported to obstruct cell proliferation, protein expression and transcriptional activity (Chantret et al. 1994; Briske-Anderson et al. 1997). We have previously shown at passages P10–P47, the glycosylation profile of Caco-2 remains essentially unaltered (Park et al. 2015). To evaluate the consequences of passage number on cell surface glycosylation, cells subcultured at earlier passages were compared to cells subcultured at later passages ($P > 80$). On average, of the 90 unique compositions identified, low passage and high passage cells shared 59 (65%) of the same glycan compositions (Figure 4C). Significant decreases of the most abundant complex and hybrid structures were apparent from low to higher passages, including $Hex_5HexNAc_5Fuc_1NeuAc_1$, $Hex_5HexNAc_5Fuc_1NeuAc_2$, $Hex_5HexNAc_5Fuc_2NeuAc_1$ and $Hex_6HexNAc_6Fuc_1$.

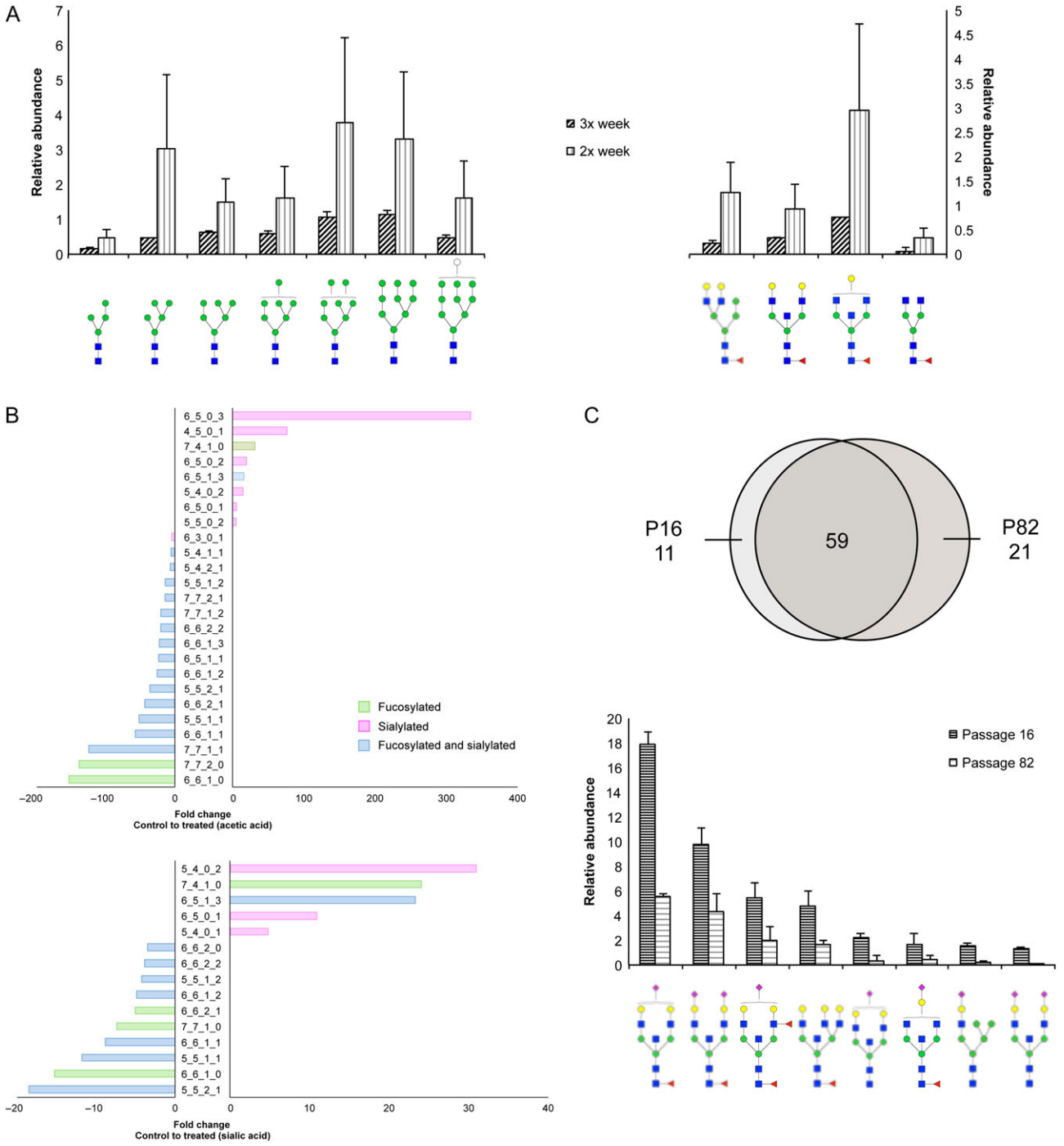

Fig. 4. Effects of growth conditions on cell surface glycans in Caco-2. (**A**) Increases in abundances in high mannose and fucosylated glycans observed when comparing cells maintained with media renewal twice or three times a week. (**B**) Fold changes of fucosylated and/or sialylated glycans in cells grown in low pH compared to cells grown in normal media. Glycan notation is as follows: Hex_HexNAc_Fuc_NeuAc. (**C**) Venn diagram indicates the number of glycan compositions identified in cells harvested at passage 16 compared to cells harvested at passage 82. Bar graph represents abundances of glycans from low passage samples that decreased compared to glycans from high passage cells. Monosaccharide symbols follow the SNFG (Symbol Nomenclature for Glycans) system details at NCBI (Varki et al. 2015). This figure is available in black and white in print and in color at *Glycobiology* online.

High mannose overexpression shapes intestinal cell membrane protein functions

Having established that exogenous factors can significantly alter cell surface *N*-glycosylation, we then interrogated whether glycan changes affect cell physiology. Due to the recurrent observations of marked changes in high mannose glycans, we examined the functional consequences of selectively increasing their expression levels. For such structure–function correlative studies, exclusivity and biocompatibility are needed. Application of an α-mannosidase I inhibitor, kifunensine, achieved nearly complete conversion into high

mannose glycans in Caco-2 without affecting viability (Figure S5). Using this approach, we subsequently analyzed cell responses in untreated and hypermannosylated cells.

Epithelial monolayer integrity is ensured by transmembrane tight junction proteins near the apical surface, where differential glycosylation may have functional influence. Paracellular permeability changes in untreated and kifunensine-treated cells were assessed in vitro by measuring the apical to basal passage of FITC conjugated dextran (FITC-D4). Cells with altered high mannose glycosylation exhibited significantly higher permeability than unaltered cells (Figure 5A). A dose-dependent effect was observed with kifunensine, which governed the extent of conversion of all surface glycans into high mannose glycans. Of note, increases in permeability were observed even without complete conversion, at 1 μg/mL treatment. After 2 h, passage of FITC-D4 from the upper to the lower chamber showed a maximum increase of 64% with 100 μg/mL treatment (untreated to treated; $P = 5.30 \times 10^{-5}$; $n = 4$). To ensure the integrity of the monolayer, we measured the transepithelial electrical resistance (TEER) before and after shaking, which showed that the transwell movement of FITC-D4 was not due to breaching of the monolayer during treatment (Figure S6).

Using comparative proteomic analysis, we and others have determined that key hydrolases associated with brush border formation, including intestinal alkaline phosphatase (IAP) and dipeptidyl peptidase IV (DPP IV), are expressed on differentiated Caco-2 cells (Stierum et al. 2003; Park et al. 2015). In this study, remodeled cells were used to examine the correlation between the proteins' glycosylation patterns and their activities. The activity of IAP measured in the enriched membrane fractions of high mannose rich cells showed a significant decrease in activity (~32%) when compared with unaltered Caco-2 cells (Figure 5B, top panel). In contrast, DPP IV activity was nearly unaffected by kifunensine treatment (Figure 5B, bottom panel). Furthermore, neither IAP nor DPP IV activity was measured in the cytoplasmic fractions.

Intestinal cell glycosylation modulates the intensity of bacterial infections

The intestinal glycocalyx mediates the first events of contact between the cell and the external environment, particularly against pathogens. We previously showed that high mannose overexpression on the host is associated with increased *Salmonella* typhimurium invasion (Park et al. 2016). To further assess the ability of different bacteria to adhere and penetrate host cells with atypical high mannose glycosylation, we infected unaltered and altered host cells with model gram negative (enterohaemorrhagic *Escherichia coli* (EHEC)) and gram positive (methicillin-resistant *Staphylococcus aureus* (MRSA)) bacterial strains that express a succession of surface proteins and secrete toxins during early encounter. Within 2 h, whereas hypermannosylation of Caco-2 did not significantly affect EHEC binding, the ability of MRSA to adhere to the monolayer increased substantially (>5000%, $P = 0.02$) (Figure 5C). This data suggests that initial attachment of bacteria is orchestrated by the "at present" extracellular *N*-glycosylation patterns of the host, which we showed can be shaped by dietary and environmental stimuli.

Adhesion and delivery of toxins is followed by bacterial entry into host cells. Both strains were moderately invasive. In comparison to control cells, EHEC uptake was significantly reduced ($P = 0.0005$) in cells that were rich in high mannose glycans as to render the interaction noninvasive. In contrast, approximately 30% more MRSA bacteria were able to invade transformed host cells than untreated cells ($P = 0.03$).

Discussion

We showed by exogenous supplementation that the amounts and types of resources made available to cells influence their displayed glycan compositions and abundances (Figure S7). Mono- and disaccharides are common additions to foods and the smallest carbohydrate units of digested material. Although the molecular structures of monosaccharides are similar, we found that the abundance of one over another can guide the synthesis of the final glycosylated products. For example, glucose alone yielded subtle changes on cell surface glycans compared to its epimer, galactose, which induced prominent increases in high mannose type glycans. Survey of the Leloir pathway in the context of galactosemia, a genetic metabolic disorder, has provided detailed insight into galactose metabolism. Gleaning from these studies, surplus galactose may have adverse effects through accumulation of metabolic intermediates or formation of alternate products such as galactitol or galactonate (Lai et al. 2009). Indeed, due to the closely integrated metabolic routes of monosaccharides, glycosylation changes are likely caused by dysregulation of more than a single pathway. However, by considering each monosaccharide individually, we observed selective responses, which inform our understanding of the precise junctures in the biosynthetic pathway that are regulated by imbalances in dietary intake. Intriguingly, while with most monosaccharide additions, we saw an effect on multiple pathways, when we introduced L-fucose, it was not converted into other monosaccharide forms before incorporating onto membrane glycoconjugates. Rather, exogenous fucose primarily affected the expression of select glycan structures that were purely fucosylated. The limited utilization of free fucose by the epithelium may in fact accentuate the beneficial effects of fucose liberation by the gut microbiota (Pickard et al. 2014).

Although biosynthesis of *N*-glycans is regulated by the bioavailability of macronutrients, cells uptake certain metabolites more readily than others. The increased availability of free per-*O*-acetylated sialic acids did not promote increased expression of sialylated products. Earlier reports on hematopoietic cell sialylation showed that incorporation of sialic acid into glycoproteins occurs from exogenous sources through a putative transporter (Oetke et al. 2001). Our results show that the efficiency of uptake may be altered by the presence of acetylation, undoubtedly an important postglycosylation modification of free sialic acids found in nature (Klein and Roussel 1998). We also note that sialic acids mostly exist as glycosidically linked forms, which may not reflect the fate of free sialic acids, as supported by the analogous but nonidentical effects of lactose and galactose treatments. Similarly, we observed low efficiency of glutamate and glutathione metabolism in differentiated Caco-2 cells. Utilization of these compounds likewise may be regulated by the activities of highly specific transporters. Glutamate is negatively charged and requires amino acid transporters that have been reported to be present at low density in the plasma membrane (Newsholme et al. 2003). Glutathione is absorbed intact through a specialized transport system separate from the intestinal peptide transport system.

Excess fructose consumption has been linked with chronic diseases and contributes to inflammation (Rayssiguier et al. 2006; Brymora et al. 2012). Our results suggest that the detrimental effects of fructose on the intestinal epithelial monolayer may be intensified by increased high mannose production. High mannose type glycans, assembled during the earlier steps of glycosylation, are minimally processed. Therefore, higher production may be dictated by factors related to postglycosylation trafficking, including impaired ability of

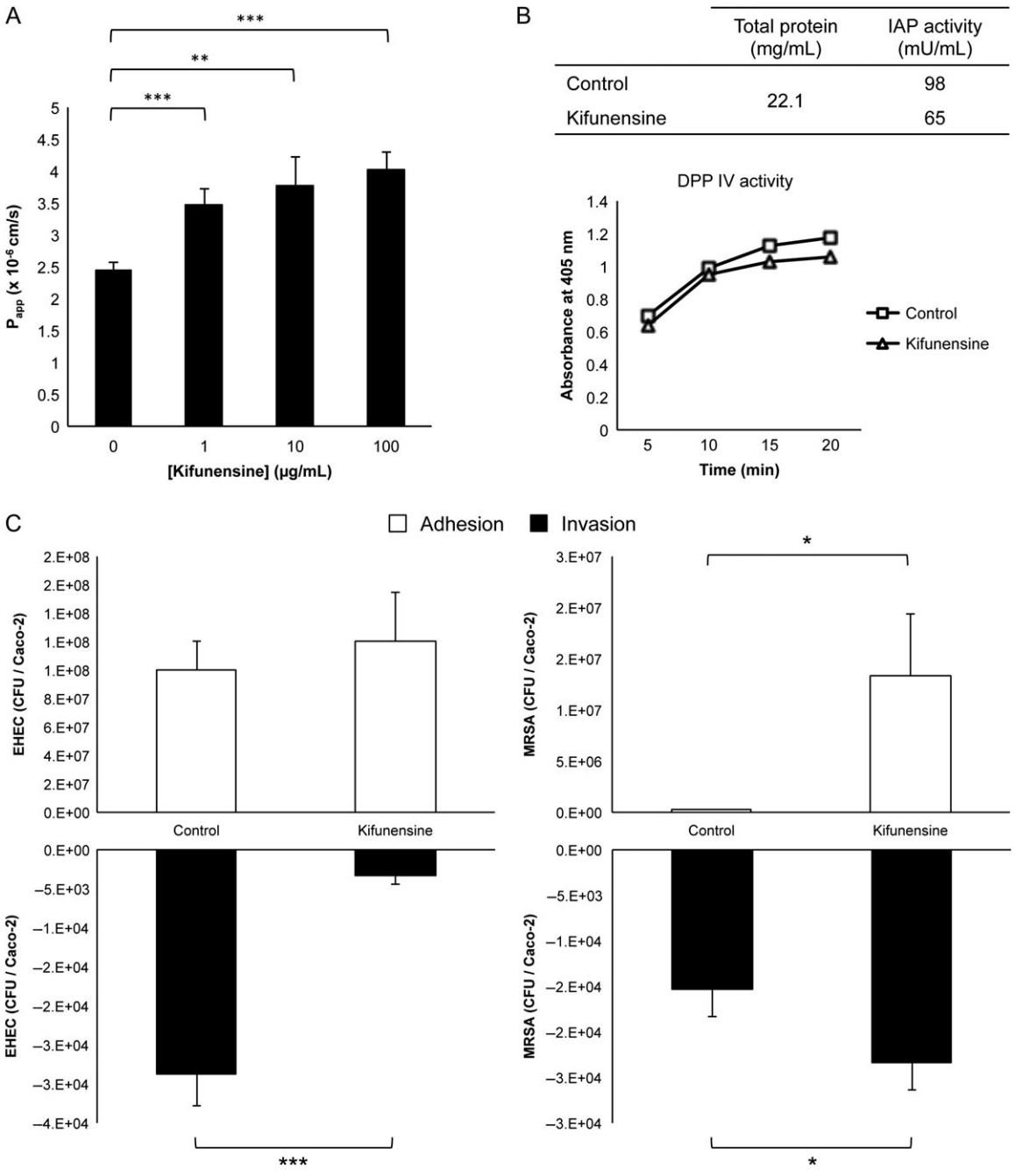

Fig. 5. Functional assays after transformation of cell surface glycans into high mannose type by kifunensine treatment. (**A**) Intensity of FITC-dextran measured in the basolateral face after passage through cell monolayers. Error bars depict standard deviation ($n = 4$). Asterisks denote statistically significant changes, where $^{**}P < 0.01$ and $^{***}P < 0.001$. (**B**) Comparison of bacterial adhesion and translocation of untreated vs. kifunensine-treated host cells. Asterisks denote statistically significant changes, where $^{*}P < 0.05$ and $^{***}P < 0.001$. (**C**) Enzymatic activity of IAP and DPP IV in membrane fractions of control and kifunensine-treated cells.

proteins to recycle through the trans-Golgi network (Parry et al. 2006). It is notable that both cell lines exhibited similar responses in the supplementation studies. However, cases where their responses were dissimilar indicate that utilization and metabolism of dietary substances are cell-dependent. HT-29, as a partially differentiated type, generally showed less intense changes in its glycome than Caco-2. Currently, studies are ongoing to track the incorporation of monosaccharides from external sources into cell- and tissue-specific biomolecules for examining nutrient distribution.

Like glucose, glutamine contributes heavily to multiple fundamental metabolic mechanisms in proliferating cells as a source of ϒ-nitrogen (as in hexosamine synthesis (Orlando et al. 2009)), α-nitrogen and carbon backbone (DeBerardinis and Cheng 2010). Accordingly, we examined the metabolic fate of glutamine in support of complex type *N*-glycan production bearing aminosugars GlcNAc and NeuAc. On the contrary, at high concentrations of supplementary glutamine, we primarily observed several fold increases in the levels of high mannose glycans. Gut mucosal barrier is dependent on steady levels of

glutamine (Souba et al. 1990; van der Hulst et al. 1993; De-Souza and Greene 2005). Absorption of glutamine in excess may provoke cells to be in a more basic environment due to the generation of ammonia during the degradation of glutamine, leading to more high mannose glycans on the surface.

An increasing number of studies describe the beneficial roles of SCFAs in barrier function, energy metabolism and immune modulation (Wong et al. 2006; den Besten et al. 2013; Correa-Oliveira et al. 2016). In the presence of low millimolar concentrations of SCFAs, Caco-2 and HT-29 cells responded similarly in favor of fucose-containing glycans. The induced increase of intestinal epithelial cell fucosylation points to the potential role of SCFAs in maintaining host-commensal symbiosis and supporting host defense against pathogens (Goto et al. 2014; Pickard et al. 2014). Additionally, we observed that varying lengths of SCFAs have different intensity of effects on cellular glycosylation, which has implications where microbial communities and SCFA distribution differ along the length of the intestines.

Intraluminal pH is adjusted by many factors such as diet, microbial byproducts and disease (Ovesen et al. 1986; Pye et al. 1990; Fallingborg 1999). Often, these factors are associated with lowering the pH. In this study, we showed that sialylated glycans dominate the surface of intestinal epithelial cells at acidic pH, which is supported by the likely enhancement of sialyltransferase activity over other glycosyltransferases (Gawlitzek et al. 2000; Ha and Lee 2014). Acidic extracellular environments have been reported to induce physiological changes such as integrin activation and metastasis (Rofstad et al. 2006; Paradise et al. 2011; Kato et al. 2013). Based on our findings, hypersialylation of proteins may be a key contributor that governs these behaviors.

The impact of glycosylation on membrane functions was evident upon transforming Caco-2 cells, which natively exhibit high levels of sialylation, into high mannose-rich cells using kifunensine. Paracellular permeability, known to be governed by tight junction proteins, was instantly impaired despite the extent of conversion. IAP showed a decline in activity after maximal high mannose conversion whereas DPP IV activity remained unaltered. As expected, glycan changes affect individual apical plasma membrane proteins differently. Two potential explanations are proposed: (i) abnormal protein glycosylation results in impaired transport to the cell surface and (ii) uniform conversion to high mannose glycosylation contribute to unsuitable protein conformations such that its functional properties are greatly reduced or lost. Loss-of-glycosylation studies have implied that a fundamental relationship exists between protein functions and proper glycosylation but often lack protein-specific information. Continuing efforts are concentrated on isolating intact glycoforms to selectively monitor individual glycoproteins and glycosites. Importantly, the consequences of glycan changes are not only observed in the cell itself but extracellularly, in the strength of bacterial interactions.

Our analysis provides details of glycomic changes induced by dietary and microbial compounds and shows that Caco-2 and HT-29 membrane glycosylation is a sensitive sensor of the cell's extracellular environment. The methods described here can be used for screening the effects of a variety of environmental changes. Cell models have limitations in that that they do not simulate the composition of the normal intestinal monolayer, which contains more than one cell type, and lack a fully formed mucus layer to separate the epithelial cell layer from the luminal content. Further progress is being made to determine whether intestinal glycosylation can be shaped by dietary supplements in vivo and whether such glycan changes contribute to gastrointestinal disturbances. Understanding the causes and effects of glycan changes has the potential to provide therapeutic strategies to strengthen barrier function by controlling local glycosylation.

Conclusion

Elements that affect the cell's intricate glycosylation pathway need to be further evaluated. The impact of cell growth conditions is dependent on a number of determinants, such as cell type, origin, species, etc. In the gut, environmental conditions can quickly vary with metabolite concentrations, pH and colonizing microbe communities. This study explores the types of environments that cause changes to the glycosylation patterns of intestinal epithelial cells. We demonstrate that unchecked dietary and bioenergetic supplements cause irregular glycosylation to occur, which indeed cause penalties to the functions and integrity of cells. These results facilitate the translation of analytical tools into physiological systems and progress toward the development of improved glycosylated products by programmed changes to relevant parameters during cell growth.

Materials and methods

Cell culture

Human colorectal adenocarcinoma Caco-2 cells, derived from a Caucasian male 72 years of age, were obtained from American Type Culture Collection (ATCC, VA) and grown in EMEM supplemented with nonessential amino acids, 2 mM L-glutamine, 10% (v/v) fetal bovine serum (Life Technologies, NY), 1 mM sodium pyruvate, 1.5 g/L sodium bicarbonate, 100 U/mL penicillin and 100 µg/mL streptomycin. Alternatively, Caco-2 cells were grown in DMEM supplemented with 10% (v/v) fetal bovine serum, 100 U/mL penicillin and 100 µg/mL streptomycin. Human colorectal adenocarcinoma HT-29 cells, derived from a Caucasian female 44 years of age, were obtained from ATCC and grown in McCoy's 5A medium supplemented with 10% (v/v) fetal bovine serum, 100 U/mL penicillin and 100 µg/mL streptomycin. Cells were subcultured at 80% confluency and maintained at 37°C in a humidified incubator with 5% CO_2. All treatments were added to the media after cell differentiation. Caco-2 cells were fully differentiated 14-days postconfluency. HT-29 cells were partially differentiated 4-days postconfluency. After 72 h, cells were collected in biological triplicates by scraping. A fixed count of 2×10^6 viable cells was used for each experiment. Passage number between experiments was controlled to no higher than P40 and a delta P of no more than 20. High passage cells were scraped after P80. Media was renewed three times a week unless specified. Monolayer integrity and quality of cell borders were evaluated under the microscope routinely during growth and before harvest (Figure S8).

Enterohaemorrhagic *E. coli* O157:H7 (EHEC) and methicillin-resistant *S. aureus* (MRSA) were grown at 37°C with continuous shaking for 14–16 h.

Permeability assay

Caco-2 cells were seeded on porous polycarbonate filter membranes (3401; Corning, NY) until cells formed a single monolayer and were fully differentiated. Kifunensine (Carbosynth, CA) was added post-differentiation for 72 h. Four replicates were prepared for both control and kifunensine-treated cases. Permeability experiments were performed in Hank's Balanced Salt Solution, prepared with 25 mM

HEPES, 0.35 g/L sodium bicarbonate, and adjusted to pH 7.4 with sodium hydroxide. The prepared membranes were washed and inserted into a new microwell plate. FITC-dextran (4 kDa) (Sigma-Aldrich, MO) was introduced to the upper (apical) chamber at 10 mg/mL. The plate was placed in a 37°C incubator devoid of CO_2 for 2 h on an orbital shaker at 100 rpm. The amount of FITC-dextran that transferred through the cells was measured in the lower (basolateral) chamber by fluorescence at 492/520 nm (excitation/emission) using a Perkin Elmer Victor3 Multilabel Plate Reader (Perkin Elmer, MA). The apparent permeability coefficient was determined according to the following equation:

$$P_{app} = \frac{dQ/dt}{AC_0}$$

where dQ/dt is the rate of permeation across cells, A is the surface area of the membrane and C_0 is the initial donor concentration. TEER values were measured using a Millicell ERS Voltohmmeter (EMD Millipore, MA) at room temperature.

Enzyme activity assay

IAP activity was measured in membrane-enriched fractions using a colorimetric assay per manufacturer's instructions (Abcam, MA). Cells were incubated with 50 μM *p*-nitrophenyl phosphate (*p*-NPP) for 60 min. Dephosphorylated was monitored by the production of *p*-nitrophenyl, which turns the solution to a visible yellow color. Absorbance readings were taken at 405 nm with a microplate photometer. Enzyme activities were determined with a standard curve generated using IAP enzyme. Activity was measured in U/mL, where a unit is defined as the amount of enzyme to hydrolyze 1 μmol of *p*-NPP per minute at 37°C.

Dipeptidyl peptidase IV (DPP IV) activity was measured in membrane-enriched fractions using a colorimetric assay per manufacturer's instructions (Enzo Life sciences, NY). Membrane extracts from control and kifunensine-treated cells were incubated with a chromogenic substrate (H-Gly-Pro-pNa) at 25°C for 30 min. Cleavage of *p*-nitroaniline (pNA) was monitored by absorbance measurements at 405 nm with a microplate photometer. Enzyme activities were compared to a standard curve generated using a pNA standard. A reaction containing a DPP IV inhibitor (P32/98) was included as a control for enzymatic specificity.

Bacterial association assay

Caco-2 cells were seeded into 24-well plates at 5×10^5 cells per well. Wells were designated as control (Row 1) or treated with kifunensine (Row 2). For adhesion, the left half of the plate was infected with logarithmically growing enterohaemorrhagic *E. coli* O157:H7 (EHEC), and the right half of the plate was infected with methicillin-resistant *S. aureus* (MRSA). Triplicate setups were prepared for each condition. After 2 h, the wells were washed 3X with PBS and the adherent cell counts were determined by serial dilutions and spotting of the lysate generated upon treatment of the wells with PBS/0.5% Triton for 5 min. CFU are expressed per mL as a comparison between the different treatments. For measuring uptake, the duplicate plate was similarly infected with EHEC and MRSA. Two hours postinfection, the unbound bacteria were washed with PBS (3X) and the Caco-2 cells were treated with media containing 100 μg/mL gentamicin to lyse cell surface associated bacteria. Following a 2 h-treatment, the internalized bacterial cell counts were derived upon lysing the Caco-2 cells with PBS/0.5% Triton followed by serial dilution and CFU counts.

Cell membrane extraction

Extraction of the cell membrane compartment was performed as described previously with modified procedures (An et al. 2012; Park et al. 2015). In brief, harvested cells were resuspended in homogenization buffer containing 0.25 M sucrose, 20 mM HEPES-KOH (pH 7.4) and 1:100 protease inhibitor (EMD Millipore, CA). Cell lysis was performed on ice using a probe sonicator (Qsonica, CT) with five alternating and on and off pulses in 5 and 10 s intervals, respectively. Lysates were centrifuged at 2000 × *g* for 10 min to remove the nuclear fraction and cellular debris. The supernatant was collected and brought to 1 mL with homogenization buffer for ultracentrifugation at 200,000 × *g* for 45 min at 4°C. The pellet was resuspended and repelleted by ultracentrifugation in 0.2 M Na_2CO_3 (pH 11) followed by water to fragment the endoplasmic reticulum and remove the cytoplasmic fraction, respectively. The resulting membrane fraction was isolated and stored at −20°C until further processing.

Enzymatic release and enrichment of *N*-glycans

Membrane pellets were resuspended with 100 μL of 100 mM ammonium bicarbonate in 5 mM dithiothreitol and heated for 10 s at 100°C to thermally denature the proteins. To cleave *N*-glycans from membrane proteins, 2 μL of peptide *N*-glycosidase F (New England Biolabs, MA) were added to the samples and incubated at 37°C in a microwave reactor (CEM Corporation, NC) for 10 min at 20 watts. After addition of 400 μL of chilled ethanol, samples were placed in −80°C for 1.5 h and centrifuged for 20 min at 21,130 × *g* to precipitate residual deglycosylated proteins. The supernatant containing the released *N*-glycans was collected and dried. *N*-Glycans were purified by solid phase extraction containing a PGC matrix. Eluted fractions were dried in vacuo.

Mass spectrometric analysis

Glycan samples were reconstituted in nanopure water for analysis using an Agilent nanoLC/ESI-QTOF-MS system (Agilent Technologies, CA). Samples were introduced into the MS with a microfluidic chip, which consists of enrichment and analytical columns packed with PGC and a nanoelectrospray tip. A binary gradient was applied to separate and elute glycans at a flow rate of 0.4 μL/min: (A) 3% (v/v) acetonitrile and 0.1% (v/v) formic acid in water and (B) 90% (v/v) acetonitrile in 1% (v/v) formic acid in water. MS spectra were acquired at 1.5 s per spectrum over a mass range of *m/z* 600–2000 in positive ionization mode. Mass inaccuracies were corrected with reference mass *m/z* 1221.991.

Collision-induced dissociation (CID) was performed with nitrogen gas using a series of collision energies ($V_{collision}$) dependent on the *m/z* values of the *N*-glycans, based on the equation:

$$V_{collision} = \text{slope}(m/z) + \text{offset},$$

where the slope and offset were set at (1.8/100 Da) V and −2.4 V, respectively.

Data analysis

N-glycan compounds were identified with an in-house retrosynthetic library of all possible glycan compositions according to accurate

mass (Kronewitter et al. 2009). Subtypes including high mannose, complex and hybrid were grouped accordingly by knowledge of the mammalian *N*-glycan biosynthetic pathway. Quantitative reproducibility and tandem MS confirmation of library matches were previously validated, enabling rapid and accurate assignment of glycan compounds (Hua et al. 2011; Ruhaak et al. 2012). Signals above a signal-to-noise ratio of 5.0 were filtered and deconvoluted using MassHunter Qualitative Analysis B.06.01 (Agilent Technologies, CA). Deconvoluted masses were compared to theoretical masses using a mass tolerance of 20 ppm and a false discovery rate of 0.6%. Area under the peak was used to represent the data. Relative abundances were determined by integrating ion counts for observed glycan masses and normalizing to the summed ion counts of all glycans detected. Statistical evaluation of significant glycan abundance changes was performed using an unpaired, two-tailed Student's *t*-test. Structures that were not observed in two of three replicates were excluded in the analysis.

Supplementary data

Supplementary data is available at *Glycobiology* online.

Conflict of interest statement

The authors declare no competing financial interests.

Funding

National Institutes of Health (R01GM049077 to C.B.L., AT007079 to D.A.M., AT008759 to D.A.M.), and the Peter J. Shields Endowed Chair in Dairy Food Science (D.A.M.).

Abbreviations

C, complex; CID, collision-induced dissociation; Fuc, fucose; Gal, galactose; GalNAc, *N*-acetylgalactosamine; Glc, glucose; GlcNAc, *N*-acetylglucosamine; H, hybrid; Hex, hexose; HexNAc, *N*-acetylhexosamine; HM, high mannose; Man, mannose; NeuAc, *N*-acetylneuraminic acid; PGC, porous graphitized carbon; PNGase F, peptide N-glycosidase F.

References

Adibi SA, Mercer DW. 1973. Protein digestion in human intestine as reflected in luminal, mucosal, and plasma amino acid concentrations after meals. *J Clin Invest*. 52:1586–1594.

Aebi M, Bernasconi R, Clerc S, Molinari M. 2010. N-glycan structures: Recognition and processing in the ER. *Trends Biochem Sci*. 35:74–82.

An HJ, Gip P, Kim J, Wu S, Park KW, McVaugh CT, Schaffer DV, Bertozzi CR, Lebrilla CB. 2012. Extensive determination of glycan heterogeneity reveals an unusual abundance of high mannose glycans in enriched plasma membranes of human embryonic stem cells. *Mol Cell Proteomics*. 11: M111.010660.

Blachier F, Boutry C, Bos C, Tome D. 2009. Metabolism and functions of L-glutamate in the epithelial cells of the small and large intestines. *Am J Clin Nutr*. 90:814S–821S.

Briske-Anderson MJ, Finley JW, Newman SM. 1997. The influence of culture time and passage number on the morphological and physiological development of Caco-2 cells. *Proc Soc Exp Biol Med*. 214:248–257.

Brymora A, Flisinski M, Johnson RJ, Goszka G, Stefanska A, Manitius J. 2012. Low-fructose diet lowers blood pressure and inflammation in patients with chronic kidney disease. *Nephrol Dial Transplant*. 27:608–612.

Chantret I, Rodolosse A, Barbat A, Dussaulx E, Brot-Laroche E, Zweibaum A, Rousset M. 1994. Differential expression of sucrase-isomaltase in clones isolated from early and late passages of the cell line Caco-2: Evidence for glucose-dependent negative regulation. *J Cell Sci*. 107(Pt 1):213–225.

Correa-Oliveira R, Fachi JL, Vieira A, Sato FT, Vinolo MA. 2016. Regulation of immune cell function by short-chain fatty acids. *Clin Transl Immunol*. 5:e73.

Cumming DA. 1991. Glycosylation of recombinant protein therapeutics: Control and functional implications. *Glycobiology*. 1:115–130.

Cummings JH, Pomare EW, Branch WJ, Naylor CP, Macfarlane GT. 1987. Short chain fatty acids in human large intestine, portal, hepatic and venous blood. *Gut*. 28:1221–1227.

De-Souza DA, Greene LJ. 2005. Intestinal permeability and systemic infections in critically ill patients: Effect of glutamine. *Crit Care Med*. 33: 1125–1135.

DeBerardinis RJ, Cheng T. 2010. Q's next: The diverse functions of glutamine in metabolism, cell biology and cancer. *Oncogene*. 29:313–324.

den Besten G, van Eunen K, Groen AK, Venema K, Reijngoud DJ, Bakker BM. 2013. The role of short-chain fatty acids in the interplay between diet, gut microbiota, and host energy metabolism. *J Lipid Res*. 54:2325–2340.

Du J, Meledeo MA, Wang Z, Khanna HS, Paruchuri VD, Yarema KJ. 2009. Metabolic glycoengineering: Sialic acid and beyond. *Glycobiology*. 19: 1382–1401.

Elliott S, Lorenzini T, Asher S, Aoki K, Brankow D, Buck L, Busse L, Chang D, Fuller J, Grant J, et al. 2003. Enhancement of therapeutic protein in vivo activities through glycoengineering. *Nat Biotechnol*. 21:414–421.

Fallingborg J. 1999. Intraluminal pH of the human gastrointestinal tract. *Dan Med Bull*. 46:183–196.

Ferraris RP, Yasharpour S, Lloyd KCK, Mirzayan R, Diamond JM. 1990. Luminal glucose-concentrations in the gut under normal conditions. *Am J Physiol*. 259:G822–G837.

Gawlitzek M, Ryll T, Lofgren J, Sliwkowski MB. 2000. Ammonium alters N-glycan structures of recombinant TNFR-IgG: Degradative versus biosynthetic mechanisms. *Biotechnol Bioeng*. 68:637–646.

Goto Y, Obata T, Kunisawa J, Sato S, Ivanov II, Lamichhane A, Takeyama N, Kamioka M, Sakamoto M, Matsuki T, et al. 2014. Innate lymphoid cells regulate intestinal epithelial cell glycosylation. *Science*. 345:1254009.

Ha TK, Lee GM. 2014. Effect of glutamine substitution by TCA cycle intermediates on the production and sialylation of Fc-fusion protein in Chinese hamster ovary cell culture. *J Biotechnol*. 180:23–29.

Helenius A, Aebi M. 2001. Intracellular functions of N-linked glycans. *Science*. 291:2364–2369.

Hilgers AR, Conradi RA, Burton PS. 1990. Caco-2 cell monolayers as a model for drug transport across the intestinal mucosa. *Pharm Res*. 7: 902–910.

Hua S, An HJ, Ozcan S, Ro GS, Soares S, DeVere-White R, Lebrilla CB. 2011. Comprehensive native glycan profiling with isomer separation and quantitation for the discovery of cancer biomarkers. *Analyst (Lond)*. 136: 3663–3671.

Hudak JE, Yu HH, Bertozzi CR. 2011. Protein glycoengineering enabled by the versatile synthesis of aminooxy glycans and the genetically encoded aldehyde tag. *J Am Chem Soc*. 133:16127–16135.

Ichikawa M, Scott DA, Losfeld ME, Freeze HH. 2014. The metabolic origins of mannose in glycoproteins. *J Biol Chem*. 289:6751–6761.

Jones DP, Coates RJ, Flagg EW, Eley JW, Block G, Greenberg RS, Gunter EW, Jackson B. 1992. Glutathione in foods listed in the National Cancer Institute's Health Habits and History Food Frequency Questionnaire. *Nutr Cancer*. 17:57–75.

Kato Y, Ozawa S, Miyamoto C, Maehata Y, Suzuki A, Maeda T, Baba Y. 2013. Acidic extracellular microenvironment and cancer. *Cancer Cell Int*. 13:89.

Keppler OT, Hinderlich S, Langner J, Schwartz-Albiez R, Reutter W, Pawlita M. 1999. UDP-GlcNAc 2-epimerase: A regulator of cell surface sialylation. *Science*. 284:1372–1376.

Kirchner S, Muduli A, Casirola D, Prum K, Douard V, Ferraris RP. 2008. Luminal fructose inhibits rat intestinal sodium-phosphate cotransporter gene expression and phosphate uptake. *Am J Clin Nutr*. 87:1028–1038.

Klein A, Roussel P. 1998. O-acetylation of sialic acids. *Biochimie*. 80:49–57.

Klimberg VS, Salloum RM, Kasper M, Plumley DA, Dolson DJ, Hautamaki RD, Mendenhall WR, Bova FC, Bland KI, Copeland EM3rd, et al. 1990. Oral glutamine accelerates healing of the small intestine and improves outcome after whole abdominal radiation. *Arch Surg*. 125:1040–1045.

Kronewitter SR, An HJ, de Leoz ML, Lebrilla CB, Miyamoto S, Leiserowitz GS. 2009. The development of retrosynthetic glycan libraries to profile and classify the human serum N-linked glycome. *Proteomics*. 9:2986–2994.

Lai K, Elsas LJ, Wierenga KJ. 2009. Galactose toxicity in animals. *IUBMB life*. 61:1063–1074.

Marcobal A, Southwick AM, Earle KA, Sonnenburg JL. 2013. A refined palate: Bacterial consumption of host glycans in the gut. *Glycobiology*. 23: 1038–1046.

Moran AP, Gupta A, Joshi L. 2011. Sweet-talk: Role of host glycosylation in bacterial pathogenesis of the gastrointestinal tract. *Gut*. 60:1412–1425.

Moremen KW, Tiemeyer M, Nairn AV. 2012. Vertebrate protein glycosylation: Diversity, synthesis and function. *Nat Rev Mol Cell Biol*. 13:448–462.

Nastasi C, Candela M, Bonefeld CM, Geisler C, Hansen M, Krejsgaard T, Biagi E, Andersen MH, Brigidi P, Odum N, et al. 2015. The effect of short-chain fatty acids on human monocyte-derived dendritic cells. *Sci Rep*. 5:16148.

Newsholme P, Lima MM, Procopio J, Pithon-Curi TC, Doi SQ, Bazotte RB, Curi R. 2003. Glutamine and glutamate as vital metabolites. *Braz J Med Biol Res*. 36:153–163.

O'Connor SE, Imperiali B. 1996. Modulation of protein structure and function by asparagine-linked glycosylation. *Chem Biol*. 3:803–812.

Oetke C, Hinderlich S, Brossmer R, Reutter W, Pawlita M, Keppler OT. 2001. Evidence for efficient uptake and incorporation of sialic acid by eukaryotic cells. *Eur J Biochem*. 268:4553–4561.

Orlando R, Lim JM, Atwood JA3rd, Angel PM, Fang M, Aoki K, Alvarez-Manilla G, Moremen KW, York WS, Tiemeyer M, et al. 2009. IDAWG: Metabolic incorporation of stable isotope labels for quantitative glycomics of cultured cells. *J Proteome Res*. 8:3816–3823.

Ovesen L, Bendtsen F, Tage-Jensen U, Pedersen NT, Gram BR, Rune SJ. 1986. Intraluminal pH in the stomach, duodenum, and proximal jejunum in normal subjects and patients with exocrine pancreatic insufficiency. *Gastroenterology*. 90:958–962.

Paradise RK, Lauffenburger DA, Van Vliet KJ. 2011. Acidic extracellular pH promotes activation of integrin alpha(v)beta(3). *PLoS One*. 6:e15746.

Park D, Arabyan N, Williams CC, Song T, Mitra A, Weimer BC, Maverakis E, Lebrilla CB. 2016. Salmonella typhimurium enzymatically landscapes the host intestinal epithelial cell (IEC) surface glycome to increase invasion. *Mol Cell Proteomics*. 15:3653–3664.

Park D, Brune KA, Mitra A, Marusina AI, Maverakis E, Lebrilla CB. 2015. Characteristic changes in cell surface glycosylation accompany intestinal epithelial cell (IEC) differentiation: High mannose structures dominate the cell surface glycome of undifferentiated enterocytes. *Mol Cell Proteomics*. 14:2910–2921.

Parry S, Hanisch FG, Leir SH, Sutton-Smith M, Morris HR, Dell A, Harris A. 2006. N-Glycosylation of the MUC1 mucin in epithelial cells and secretions. *Glycobiology*. 16:623–634.

Pickard JM, Maurice CF, Kinnebrew MA, Abt MC, Schenten D, Golovkina TV, Bogatyrev SR, Ismagilov RF, Pamer EG, Turnbaugh PJ, et al. 2014. Rapid fucosylation of intestinal epithelium sustains host-commensal symbiosis in sickness. *Nature*. 514:638–641.

Pinto M, Robineleon S, Appay MD, Kedinger M, Triadou N, Dussaulx E, Lacroix B, Simonassmann P, Haffen K, Fogh J, et al. 1983. Enterocyte-like differentiation and polarization of the human-colon carcinoma cell-line Caco-2 in culture. *Biol Cell*. 47:323–330.

Pye G, Evans DF, Ledingham S, Hardcastle JD. 1990. Gastrointestinal intraluminal pH in normal subjects and those with colorectal adenoma or carcinoma. *Gut*. 31:1355–1357.

Rasmussen JR. 1992. Effect of glycosylation on protein function. *Curr Opin Struct Biol*. 2:682–686.

Rayssiguier Y, Gueux E, Nowacki W, Rock E, Mazur A. 2006. High fructose consumption combined with low dietary magnesium intake may increase the incidence of the metabolic syndrome by inducing inflammation. *Magnes Res*. 19:237–243.

Rofstad EK, Mathiesen B, Kindem K, Galappathi K. 2006. Acidic extracellular pH promotes experimental metastasis of human melanoma cells in athymic nude mice. *Cancer Res*. 66:6699–6707.

Rousset M. 1986. The human colon carcinoma cell lines HT-29 and Caco-2: Two in vitro models for the study of intestinal differentiation. *Biochimie*. 68:1035–1040.

Ruhaak LR, Miyamoto S, Kelly K, Lebrilla CB. 2012. N-Glycan profiling of dried blood spots. *Anal Chem*. 84:396–402.

Ruhaak LR, Taylor SL, Miyamoto S, Kelly K, Leiserowitz GS, Gandara D, Lebrilla CB, Kim K. 2013. Chip-based nLC-TOF-MS is a highly stable technology for large-scale high-throughput analyses. *Anal Bioanal Chem*. 405:4953–4958.

Sackstein R. 2012. Glycoengineering of HCELL, the human bone marrow homing receptor: Sweetly programming cell migration. *Ann Biomed Eng*. 40:766–776.

Snider MD. 2002. Metabolic labeling of glycoproteins with radioactive sugars. *Curr Protoc Cell Biol*. Chapter 7:Unit 7.8.

Souba WW, Klimberg VS, Plumley DA, Salloum RM, Flynn TC, Bland KI, Copeland EM3rd. 1990. The role of glutamine in maintaining a healthy gut and supporting the metabolic response to injury and infection. *J Surg Res*. 48:383–391.

Stierum R, Gaspari M, Dommels Y, Ouatas T, Pluk H, Jespersen S, Vogels J, Verhoeckx K, Groten J, van Ommen B. 2003. Proteome analysis reveals novel proteins associated with proliferation and differentiation of the colorectal cancer cell line Caco-2. *Biochim Biophys Acta*. 1650:73–91.

Stowell SR, Ju T, Cummings RD. 2015. Protein glycosylation in cancer. *Annu Rev Pathol*. 10:473–510.

Tailford LE, Crost EH, Kavanaugh D, Juge N. 2015. Mucin glycan foraging in the human gut microbiome. *Front Genet*. 6:81.

van der Hulst RR, van Kreel BK, von Meyenfeldt MF, Brummer RJ, Arends JW, Deutz NE, Soeters PB. 1993. Glutamine and the preservation of gut integrity. *Lancet*. 341:1363–1365.

Varki A, Cummings RD, Aebi M, Packer NH, Seeberger PH, Esko JD, Stanley P, Hart G, Darvill A, Kinoshita T, et al. 2015. Symbol nomenclature for graphical representations of glycans. *Glycobiology*. 25: 1323–1324.

Vermeulen MA, de Jong J, Vaessen MJ, van Leeuwen PA, Houdijk AP. 2011. Glutamate reduces experimental intestinal hyperpermeability and facilitates glutamine support of gut integrity. *World J Gastroenterol*. 17: 1569–1573.

Wong JM, de Souza R, Kendall CW, Emam A, Jenkins DJ. 2006. Colonic health: Fermentation and short chain fatty acids. *J Clin Gastroenterol*. 40:235–243.

Wurm FM. 2004. Production of recombinant protein therapeutics in cultivated mammalian cells. *Nat Biotechnol*. 22:1393–1398.